THERMAL PERFORMANCE OF A RECEIVER LOCATED IN THE CAUSTIC AREA OF A CYLINDRO-PARABOLIC SOLAR CONCENTRATOR

B. M. Pakouzou[1, 2*], T.S.M. Ky[2], S. T. Gbembongo[1, 3], W. G. Ouedraogo[2], O. A. Mackpayen[1], B. Dianda[2], S. Kam[2], D. J. Bathiebo[2*]

[1]Carnot Laboratory of Energetics, Faculty of Sciences, University of Bangui, C.A.R

[2]Laboratory of Renewable Thermal Energies, University Ouaga1 Prof. Joseph KI-ZERBO, Burkina Faso.

[3]Laboratory of Mathematics and Physics of Systems-Mechanics and Energetics Group, France.

djbathiebo@gmail.com and mb.pakouzou@gmail.com

SUMMARY: Indirect solar dryers with solar collectors, do not always make it possible to reach the desired temperature level and drying time. As part of the improvement of the thermal performance of these systems, a study of the caustic zone is first presented. It is in this zone that the tubular receiver of the studied insolator is placed. The system of equations obtained results from the division of the insolator into fictitious slices of length dz, in which the thermal balance is established. It is solved using an iterative method with finite differences. The volumetric flow rate and the temperature of the heat transfer fluid which can be injected into the drying cage during a day are thus determined at the outlet.

Keywords: Receiver; Solar; Caustic; Cylindro-parabolic; Finite difference; Modelization; Flow

NOMENCLATURES

A_i : area of a slice [m^2]

C_i : specific heats [$J.kg^{-1}.K^{-1}$]

C_g : geometric concentration

D_i : diameters [m]

dz : length of a slice [m]

f : focal length [m]

F : stove

Gr : Grashoff's number

* Corresponding authors

h_i : transfer coefficients [$W/m^2.K$]

HJ : enthalpy of dry air [kJ/kg.ASA]

I : direct solar radiation [W/m^2]

K : number of nodes along z-axis

K_{eff} : effective conductivity of air [$W/m^2.K$]

L : total length of the receiver [m]

Nu : Nusselt's number

p : parameter of the parabola

P : power at the collector [W]

Pr : Prandlt's number

Ra : Rayleigh's number

Rac : Simplified Rayleigh

q_a : absorbed flux [W/m]

q_m : mass flow [$kg.s^{-1}$]

q_v : volume flow [$m^3.s^{-1}$]

q_w : flux gained by the removable fluid [W/m]

Sc : Collector area [m^2]

T_i : Temperatures [K]

V_m : average air speed [$m.s^{-1}$]

GREEK LETTERS

α : absorptivity [%],

β : thermal expansion coefficient [1/K]

δ : angle [rad]

ε : emissivity [%]

θ : angle [rad]

κ : angle [rad]

λ_i : thermal conductivity coefficient [$W.m^{-1}.K^{-1}$]

μ : angle [rad]

ν : kinematic viscosity [$m^2.s^{-1}$]

ρ_i : densities [$kg.m^{-3}$]

σ : Stefan's constant [$W.m^{-2}.K^{-4}$]

τ : transmitivity [%]

φ_1 : heat flow [W]

1. INTRODUCTION

Solar drying is a well-suited conservation technique in countries with high levels of sunlight such as Burkina Faso (5.5 to 6.5 kWh / m² / day) [1] and the Central African Republic (4.8 kWh / m^2 / day). Indirect solar dryers do not always have the desired thermal performance. Numerous studies have been carried out in order to improve temperature level and drying time in indirect solar systems by optimizing the thermal performance of the insolators placed upstream of the drying cage.

Mohamad A. [2] presents an analysis for a new type of solar air heater. The main idea is to minimize heat losses from the front cover of the collector and to maximize heat extraction from the absorber. This can be done by forcing air to flow over the front glass cover (preheat the air) before passing through the absorber. The analysis indicates that the suggested heater thermal efficiency can exceed 75% but remains expensive. Kolb A. et al. [3] carried out experimental studies on a solar air collector with metal matrix absorber. The absorber of the collector consists of two parallel sheets of black oxidized or black galvanized industrial woven, fine-meshed wire screens made of copper. The new matrix collector efficiency is about 81% but the manufacturing costs are very high. Abene A. et al. [4] measured the drying time of grapes to the required moisture content with a constant air flow rate. Measurement time without obstacles in the flat plate collector is 13h20 min and with transverse-longitudinal obstacles in the collector is 5h50min. The introduction of obstacles in the air channel is an important factor for the improvement of collector performance which in turn reduces the drying time of grapes.

Dianda et al. [5] fixed straight fins on a solar absorber and found an improvement up to 20% of the thermal efficiency. Aoues K. et al. [6] carried out a comparative study on two thin baffle configurations welded to the absorber of solar collectors, spaced 10 cm apart for one and 5 cm for the other and tilted at an angle of 60° in comparison to the direction of the flow of the heat transfer fluid. These two configurations, A_1 and B_1, are differentiated by the number of rows of baffles, respectively equal to 152 and 256.

This comparison shows that the best configuration, B_1, is the one giving the highest thermal efficiency that is 57.80%. Blake R. et al. [7] investigated the effectiveness of adding a cylindro-parabolic solar concentrator built from low-cost, locally available materials to a typical Tanzanian solar crop dryer. Two identical solar crop dryers were constructed, with one serving as the control and the other for testing the solar concentrator. The tomatoes in the dryer with the concentrator, reached the 10% moisture content level at 1.54 h, or 22.3% faster than those

in the control dryer. Henaoui M. et al. [8] simulated an air flow in a solar collector equipped with perforated rectangular baffles, fixed alternately on the absorber and the thermal insulator. The turbulent flow thus caused, results in temperature variations of 37°C in comparison to the ambient due to the slowing down of heat transfer fluid recirculation speed at the ends of the baffles.

The choice of a concentrating collector as an air insolator constitutes a viable technico-economic compromise avoiding the pitfall associated with the costs of improving the thermal performance of a solar collector, and of course, an alternative to the low energy density of incident solar radiation [9]. The increase of temperature level increases the drying air efficiency, and consequently the drying rate [10]. Following the photograph of the device constructed in Fig. 1, we first present the zone of caustics obtained during a typical day in Ouagadougou. Subsequently, we simulate the thermal performances of an insolator, consisting of a parabola equipped with a receiver, placed in the center of caustics zone. It is noted that this always encompasses the stove. The whole is inclined by 13° above the horizontal, in order to favor the flow in natural convection of hot air.

2. CAUSTICS OF CYLINDRO-PARABOLIC REFLECTORS

Here, *caustic* is the curve in which the rays reflected (*caustic cata*) or refracted (*dia caustic*) are collected. These rays have there a burning force, see annex [11]. Figure 2 shows the caustics obtained during a typical day between 8:00 and 16:00, that is, $-60° < \mu < +60°$, like the incidence angle of sun's rays.

It permits to confirm that the suitable zone where to place our receiver is around the stove.

Fig. 1. Photo of the experimental device

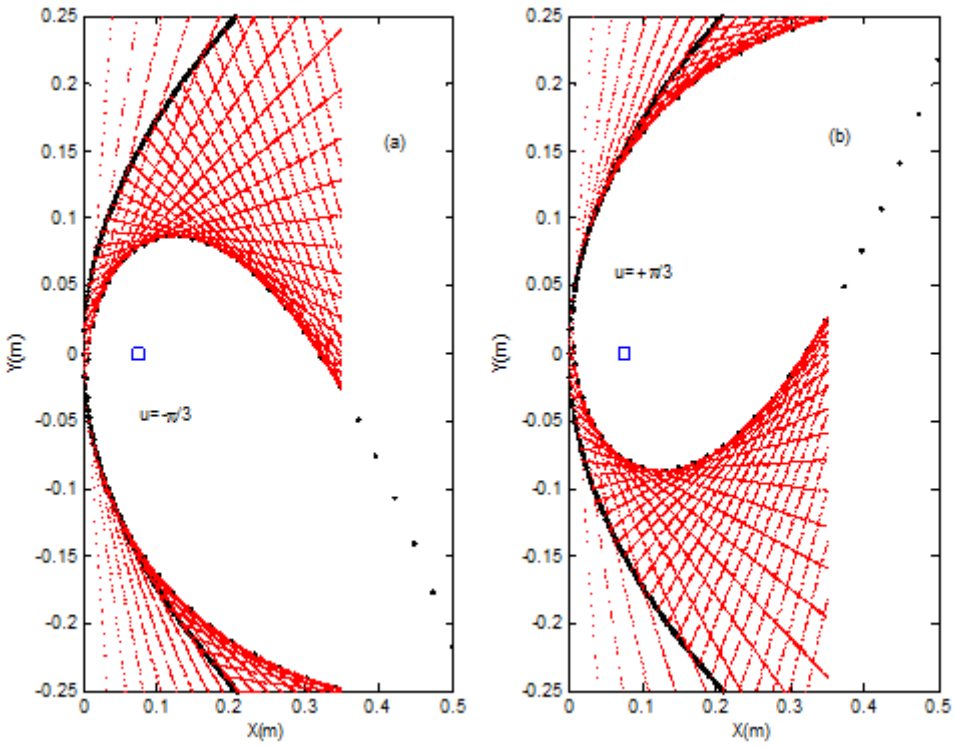

Fig. 2. Extreme Caustics μ=-60° et μ=+60°

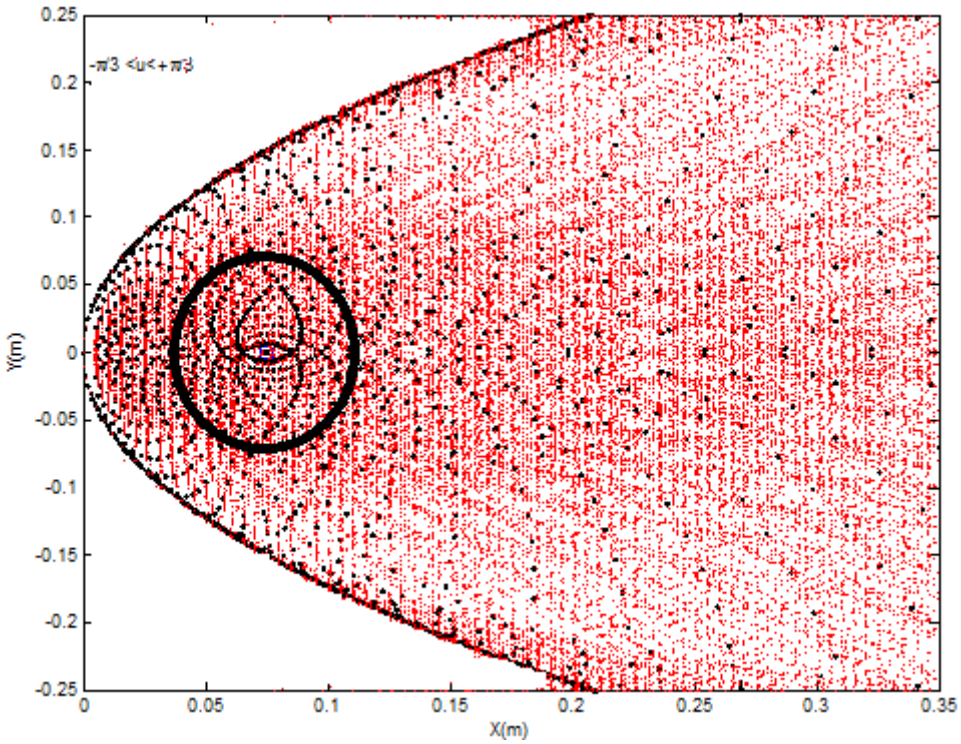

Fig. 3. Caustics for -60° < μ < +60°

3. FORMULATION OF THE PROBLEM

We use a parabola of aperture a = 0.5m, of focal length, f = 0.10m. The receiver consists of a tube 10 cm in diameter and 1 m long, placed as shown in Fig. 1. The receiver is made up of two coaxial cylindrical tubes, the first is made of glass and provides the greenhouse effect and the second, in blackened steel, acting as absorber of the reflected solar flux. The whole is tilted at an angle of 13° in comparison to the horizontal to favor the movements of natural convection towards the outlet. The purpose of the analysis of the heat transfer within the system is to determine the temperatures and the air flow at the outlet for a given solar irradiation.

4. TRANSFER EQUATIONS

The receiver in the form of a cylindrical tube, covered with a glass envelope, placed in the stove of the concentrator, comprises an absorber made of a metal black-painted metal, which absorbs the reflected solar flux and then converts it into heat. This heat is transmitted to the drying air, which circulates inside the absorber by natural convection. Thermal flow analysis is a fundamental step in improving the overall system performance. Under assumption that the

temperature is constant at circumference of absorber, the different exchanges of heat in the absorber are distributed as follows:

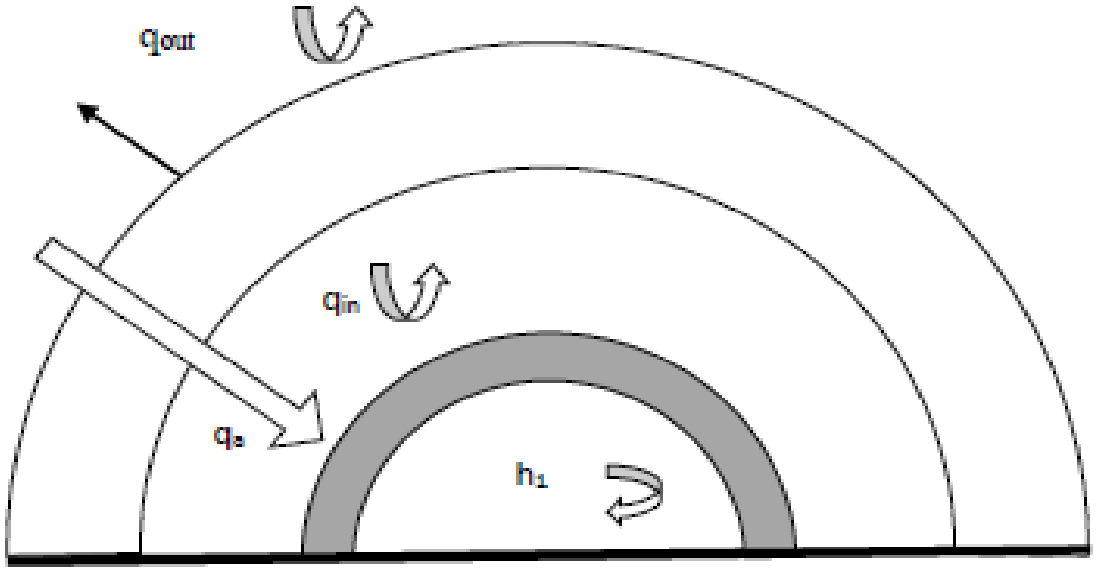

Fig. 4. Cross section of the heat transfer tube

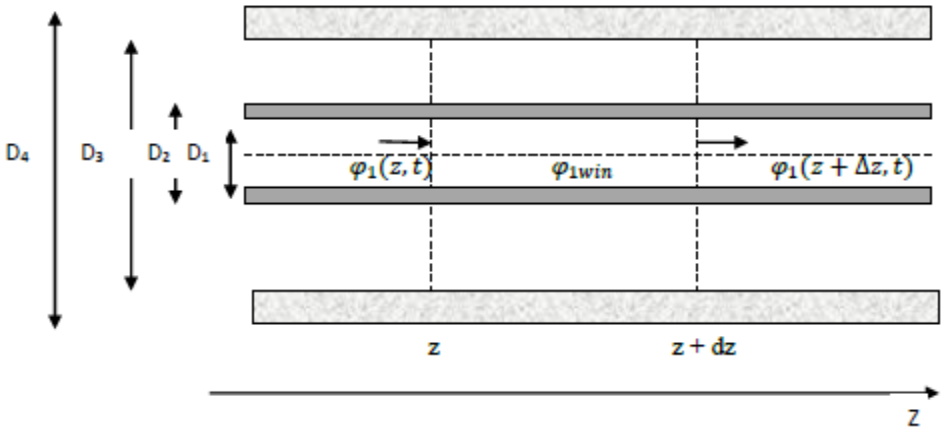

Fig. 5. Longitudinal section of heat transfer tube

4.1 Transfer of heat between the absorber and the heat transfer fluid

Following [12], we examine here the natural convection between the wall of the absorber and the heat transfer fluid. The variation of heat of the heat transfer fluid during a time t in an element of length dz at the position z of the absorber tube is given by the following equations:

$$\Delta Q_1(z,t) = \rho_1 C_1 A_1 \Delta z T_1(z,t) \quad (1)$$

$$\frac{\partial Q_1(z,t)}{\partial t} = \rho_1 C_1 q_V T_1(z,t) \quad (2)$$

Then thermal balance becomes, at time t, in the element of length dz:

$$\frac{\partial(\Delta Q_1(z,t))}{\partial t} = \varphi_1(z,t) - \varphi_1(z+\Delta z,t) + \varphi_{1Win}(z,t) \quad (3)$$

with,

$$\varphi_{1Win}(z,t) = q_W \Delta z\,, \quad (4)$$

$$\varphi_1(z,t) = \frac{\partial Q_1(z,t)}{\partial t} = \rho_1 C_1 q_V T_1(z,t), \text{ thermal power yielded to the fluid} \quad (5)$$

$$\varphi_1(z+\Delta z,t) = \rho_1 C_1 q_V T_1(z+\Delta z,t), \text{ thermal power lost by the fluid} \quad (6)$$

Then equation (3) becomes:

$$\rho_1 C_1 A_1 \frac{\partial T_1(z,t)}{\partial t} = -\rho_1 C_1 q_V \frac{\partial T_1(z,t)}{\partial z} + q_w(z,t) \quad (7)$$

q_w is calculated as follows:

- Rayleigh number is first calculated

$$Ra_1 = \frac{g\beta(T_2 - T_1){D_1}^3}{\nu\alpha};$$

$$Nu_1 = 0.6(Ra_1 * sin\theta)^{0.25}\,, [13]; \quad (8)$$

Then we have $h_1 = \frac{Nu_1 \lambda_a}{\nu\alpha}$

The solution, T_1 (z, t), represents the variation of the drying air temperature, circulating inside the channel. $q_w(z,t) = h_1 \pi D_1 (T_2 - T_1)$ represents the heat transmitted to the heat transfer fluid by natural convection.

4.2 Thermal analysis of the absorber

The thermal balance of the receiver is given by:

$$\rho_2 C_2 A_2 \frac{\partial T_2(z,t)}{\partial t} = \lambda_2 A_2 \frac{\partial^2 T_2(z,t)}{\partial z^2} + q_a(z,t) - q_{in}(z,t) - q_w(z,t) \quad (9)$$

which solution is the temperature of the receiver, T_2 (z, t), where the absorbed flux, q_a, by the slice dz of the receiver is defined by:

$$q_a(z,t) = I \times (\rho \tau_3 \alpha_2) \times C_g \times A_2 / dz \quad (10)$$

with dz = (L/K).

$q_{in}(z,t)$ represents the energy exchanged by convection assimilated to a conduction comprising a corrective coefficient k_{eff} and by radiation, respectively, through the air confined between the absorber and the glass (greenhouse effect).

The effective thermal conductivity,

$$k_{eff} = \max\left(1,\ 0.386 \times (\mathrm{Pr} \times Rac/(0.861 + \mathrm{Pr}))^{0.25}\right), \quad (11)$$

With:

$$q_{in}(z,t) = \frac{2\pi K_{eff}}{\ln\left(\frac{D_3}{D_2}\right)}(T_2 - T_3) + \frac{\sigma \pi D_2 \left(T_2^4 - T_3^4\right)}{\frac{1}{\varepsilon_2} + \frac{1-\varepsilon_3}{\varepsilon_3}\left(\frac{D_2}{D_3}\right)} \quad (12)$$

4.3 Heat exchange between the glass, the absorber and the outside

These exchanges are made by natural convection, by calling T_3 (z, t) the temperature of the transparent cover of the receiver, the heat exchange between it and the atmosphere is established by the following equality:

$$\rho_3 C_3 A_3 \frac{\partial T_3(z,t)}{\partial t} = \lambda_3 A_3 \frac{\partial^2 T_3}{\partial z^2} + q_{in}(z,t) - q_{out}(z,t) + q_b(z,t) \quad (13)$$

q_{out}, amount of heat exchanged between the glass cover and the external environment.

$$q_{out}(z,t) = h_4 \pi D_4 (T_3 - T_{amb}) + \varepsilon_3 \pi \sigma D_4 \left(T_3^4 - T_{amb}^4\right) \quad (14)$$

$$q_b(z,t) = I \times (\rho \alpha_3) \times C_g \times A_3 / dz \quad (15)$$

The system of algebraic equations consists of three equations:

$$\begin{cases} \rho_1 C_1 A_1 \dfrac{\partial T_1(z,t)}{\partial t} = -\rho_1 C_1 q_V \dfrac{\partial T_1(z,t)}{\partial z} + h_1 \pi D_1 \left(T_2 - T_1\right) \\ \rho_2 C_2 A_2 \dfrac{\partial T_2(z,t)}{\partial t} = \lambda_2 A_2 \dfrac{\partial^2 T_2(z,t)}{\partial z^2} + q_a(z,t) - h_2\left(T_2 - T_3\right) - h_3\left(T_2^4 - T_3^4\right) - h_1 \pi D_1 \left(T_2 - T_1\right) \\ \rho_3 C_3 A_3 \dfrac{\partial T_3(z,t)}{\partial t} = \lambda_3 A_3 \dfrac{\partial^2 T_3(z,t)}{\partial z^2} + h_2\left(T_2 - T_3\right) + h_3\left(T_2^4 - T_3^4\right) - h_4 \pi D_4 \left(T_3 - T_{amb}\right) - h_5\left(T_3^4 - T_{amb}^4\right) + q_b(z,t) \end{cases} \quad (16)$$

5. DISCRETIZATION

The method of progressive finite differences is chosen for the discretization of the system, which is transformed in matrix form below; the details of the discretization are appended.

$$\begin{pmatrix} F_3 & -h_{12} & 0 \\ -h_{12} & G_3 & -h_6 \\ 0 & -h_6 & H_3 \end{pmatrix} \begin{pmatrix} T_1(j,n+1) \\ T_2(j,n+1) \\ T_3(j,n+1) \end{pmatrix} = \begin{pmatrix} F_6 \\ G_7 \\ H_9 \end{pmatrix} \quad (17)$$

The method of resolution is as follows:

a) First, the various heat exchange coefficients, hi, between the various elements characterized by their arbitrarily fixed temperature, are calculated using the usual correlations employed in thermal convection.

b) The new temperatures are then recalculated from hi values thus found (Gauss Seidel)

c) These lead to new values of hi coefficients and so on until the IT-1 iteration temperature values are practically equal to those obtained at the iteration IT

$$\left|T_{(j,n+1)}^{IT} - T_{(j,n+1)}^{IT+1}\right| < 10^{-3} \quad (18)$$

6.VOLUMETRIC FLOW OF HOT AND DRY AIR

The air flow moved easier by natural convection inside the tilted tube, compared to the horizontal one. The expression of the fluid speed is obtained, by using the approximation of Boussinesq, in [13];

$$V = \frac{\beta D_1^{\,2}}{8\nu}\left(T_2 - T_1\right)\left[1 - \left(\frac{z}{D_1/2}\right)^2\right] g \sin\theta \quad (19)$$

The tube being cylindrical:

$$V_m = \frac{1}{D_1}\int_{-D_1/2}^{D_1/2} V dz \qquad \Rightarrow \qquad V_m = \frac{\beta D_1^{\,2}}{24\nu} g \sin\theta\left(T_2 - T_1\right) \tag{20}$$

$$q_v = V_m \times S \qquad \Rightarrow \qquad q_v = \frac{\beta g}{6\pi\nu} g \sin\theta\left(T_2 - T_1\right) \tag{21}$$

7. VALIDATION OF CALCULATION CODE

The simulation program, with the Matlab software (R2015a), for sunshine measured continuously on September 12, 2017 permits to compare the temperatures in experimental outlets with those obtained by our calculation code.

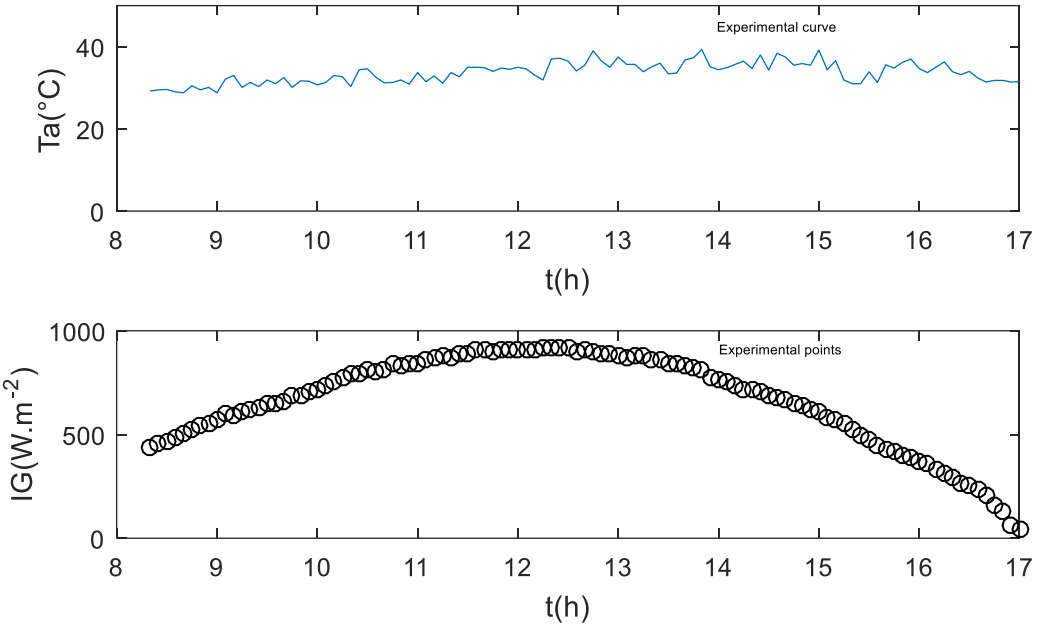

Fig. 6. Evolution of ambient temperature and irradiation according to the time

These data, on ambient temperature and irradiation are introduced in our calculation code. In order to validate it, we compare the temperatures calculated with the code to those measured experimentally. Our criterion of assessment is obtained by evaluating the average systematic error; RMSE = $\sqrt{\frac{1}{N}\sum_{i=1}^{N}(T_{1i} - T_{1,sim})^2}$ = 4.5°C, (figure 7).

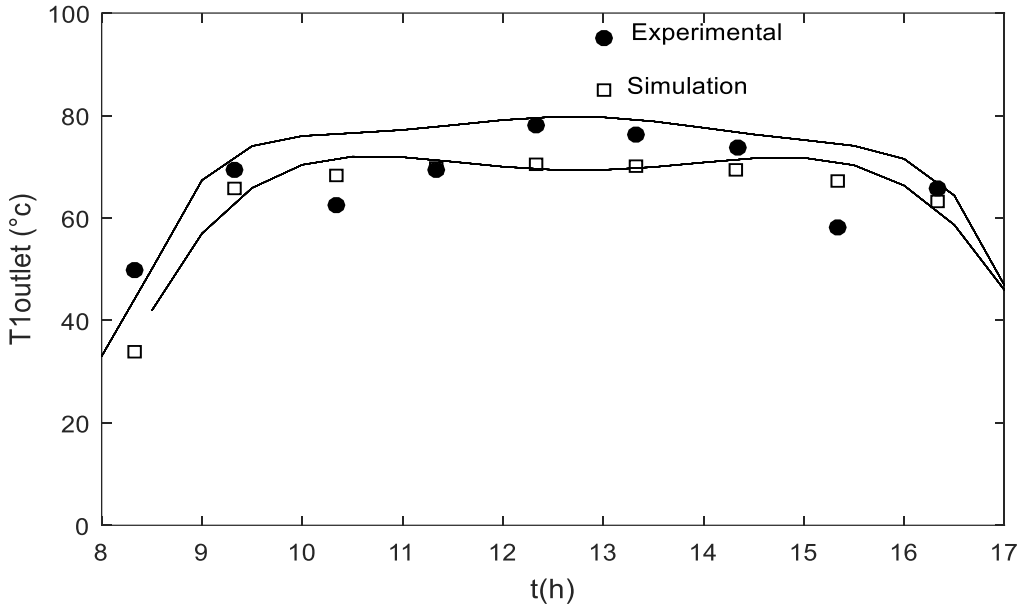

Fig. 7. Evolution of fluid temperature at the inlet of the drying chamber

The calculation code used allowed us to simulate the evolution of temperatures in the tube according to the time.

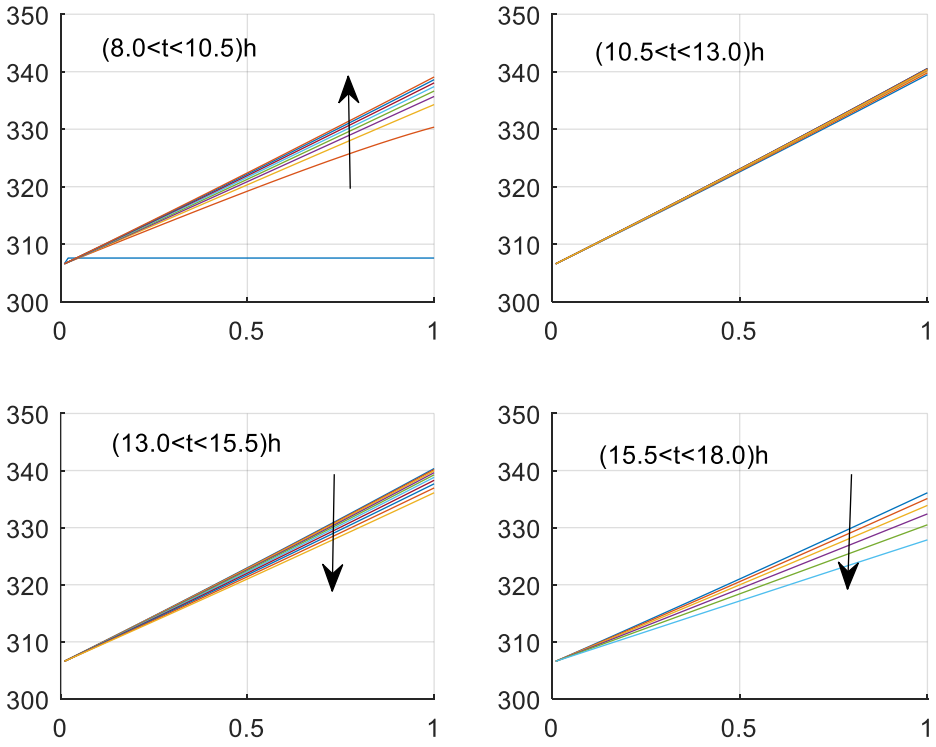

Fig. 8. Evolution of the fluid temperature during the day

In figure 8, at the beginning of the day, (8.0< t <10.0) h, temperatures increase linearly and then stabilize along the axis of the absorber tube. Between (10.5< t <13.0) h, the flow is fully developed in the tube and the fluid reaches its maximum temperature. Between (15.0< t <18.0) h, sun irradiance is attenuated and the temperatures of the fluid decrease of course in the absorber.

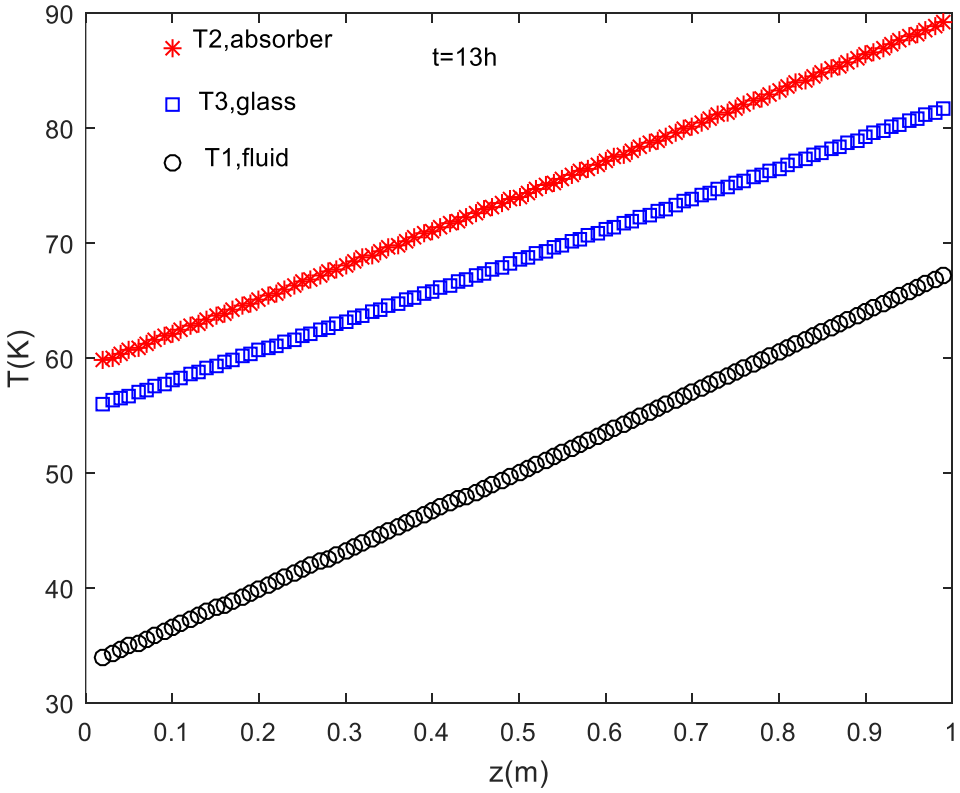

Fig.9: **Evolution of glass, fluid and absorber temperatures**

Fig.9 illustrates the evolution of the various materials of the receiver. As soon as the concentrator is exposed to the solar flux, the different elements (fluid, absorber, glass) constituting the receiver, heat up of course faster than the heat transfer fluid and very quickly reach final temperatures of approximately 90°C at the outlet of the tube, with a concentrator of 0.5 m² of useful surface. We notice that these temperatures have the same progression. The temperatures of the absorber and of the glass are, of course, higher than that of the fluid which nevertheless exceeds 67 ° C.

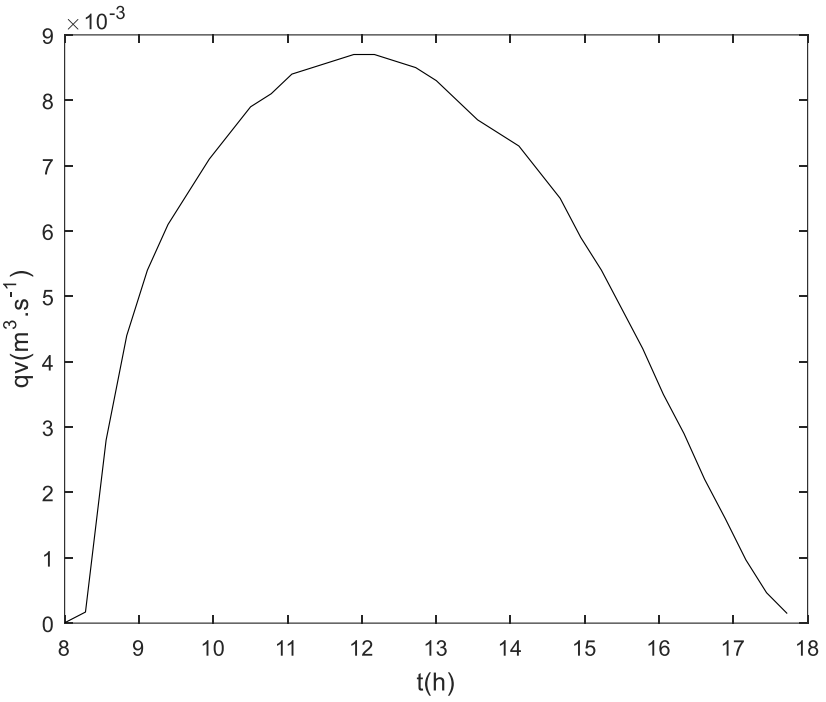

Fig. 10. Evolution of the air flow going into the drying cage

Of course, it is also observed that the flow varies as the intensity of sun irradiance. It is remarkable to have practically a flow of 9.10^{-3} $m^3.s^{-1}$ between 12:00 and 13:00 in natural convection. Such flow rates increase the drying process since the convective exchange coefficients increase according to the speed of the flow. This phenomenon is reflected in the evolution of Nusselt's number in the tube.

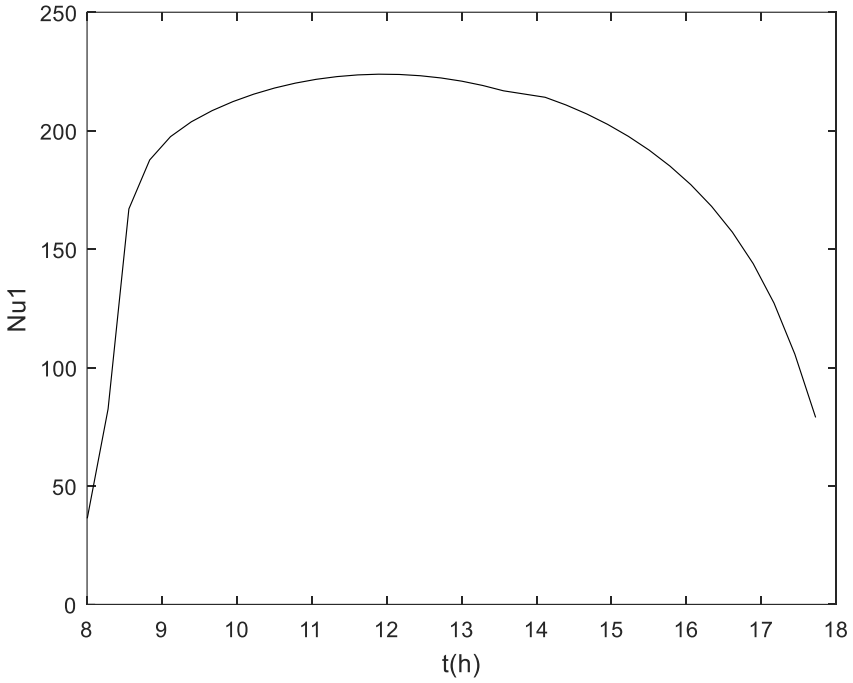

Fig. 11. Evolution of Nusselt's number in the heat transfer fluid

Figure 11 shows that the level of thermal exchanges is very high at 8:30. This level stays at the maximum from 9:00 to 15:00. This important thermal exchange of the studied system permits to substantially reduce the dimensions of the receiver, compared to conventional solar dryers with solar energy collectors.

8. CONCLUSION

We carried out an experimental study on the thermal performances of a receptor dimensioned and placed, starting from the analysis of the caustics of parabolas. The numerical model for calculation of free-convective flow and heat transfer was developed.

Initially and to validate our model, we compare the temperatures of the air on the outlet side of the absorber obtained in experiments and simulated. The simulation obtained using our computer code is satisfactory, within sight of the RMSE equal to 4.5°C.

Between (10.5< t <13.0) h, the convective flow is fully developed in the tube and the fluid reaches its maximum temperature.

Hot air flow reached 9.10^{-3} $m^3.s^{-1}$ between 12:00 and 13:00 in natural convection.

Evolution of Nusselt's number in natural convection, shows an important thermal exchange of the studied system between 09:00 and 16:00

This study can constitutes a first approach in the conception of the receiver of a cylindro-parabolic solar collector.

ACKNOWLEDGEMENTS

The ISP, Uppsala University, Sweden is gratefully acknowledged for their support to project BUF01.

REFERENCES

1. OUSMAN M. et al. Experimental Study in Natural Convection. Global Journal of Pure and Applied Sciences. 2015; 21(2):155. DOI: 10.4314/gjpa.v21i2.8.
2. MOHAMAD A. A. High Efficiency Solar Air Heater. Mechanical Engineering Department, Eastern Mediterranean University, G. Magosa, North Cyprus, Mersin 10, Turkey Solar Energy Vol. 60 (2),1997; pp. 71-76.
3. KOLB A.et al. Experimental studies on a solar air collector with metal matrix absorber Solar Energy, Vol.65 (2), 1999; pp. 91-98. DOI 10.1016/S0038-092 X (98)00117-0.
4. ABENE A. et al. Study of a solar air flat plate collector: Use of obstacles and application for the drying of grape, jfoodeng.2003.11.002, DOI: 10.1016/j.
5. DIANDA B. et al. Experimental study of the kinetics and shrinkage of tomato slices in convective drying. African Journal of Food Science Vol. 9 (5), 2015; pp. 262-271, DOI: 10.5897/AJFS2015.1298 Article Number: 2C40F1F53019 ISSN 1996-0794.
6. AOUES K.et al. Amélioration des Performances Thermiques d'un Capteur Solaire Plan à Air: Etude Experimentale Dans La Region De Biskra, Magister de l'Université de Biskra, CDER (Centre Des Energies Renouvelables) Alger, 2009.
7. BLAKE R. et al. Concentrated Solar Drying of Tomatoes**.** University Energy for Sustainable Development. Energy for Sustainable Development 19, 2014; pp. 47–55, doi.org/10.1016/j.esd.2013.11.006.
8. PAKOUZOU B. M. et al. Conception d'un Capteur Cylindro-Parabolique Appliqué à Un Séchoir Solaire Agricole. 16èmes Journées Internationales de Thermique (JITH 2013), Marrakech (Maroc), du 13 au 15 Novembre, 2013.
9. ILHEM Z. Etude et Réalisation d'un Concentrateur Solaire Parabolique. Mémoire de Magister, Université Mentouri – Constantine, 2005.
10. LUQUE M. Caustique de Miroirs Paraboliques et Sphériques, Manuel Luque. Éditions Jacques Gabay, Paris, 2010.

11. TOUATI B. Etude Théorique et Expérimentale du séchage solaire des feuilles de la Menthe Verte (Mentha Viridis), thèse de doctorat, Université de Tlemcen, Algérie, 2008.
12. CHEKIROU W. et al. Différents modes de transfert de chaleur dans un absorbeur d'un concentrateur solaire cylindro-parabolique. Revue des Energies Renouvelables ICRESD-07 Tlemcen, 2007; pp. 21-28.
13. BEJAN A. Convection heat transfer, John Wiley & Sons, ISBN 0-471-27150-0, New-York (USA), 2004.

ANNEX

Determination of collector's caustic equations

The construction of cata caustic is based on the following property: if μ is the inclination of incident rays with the axis of the parabola, then « *the reflected ray* (IR) *makes with the vector ray* (IF) *the constant angle* μ » [10].

Let us determine angle k, made by (IR) with (OX). (x_I, y_I) are the coordinates of the point on the parabola.

If $\delta = -\arctan\left(\frac{y_I}{\frac{p}{2} - \frac{y_I^2}{p}}\right) + \pi$ (A1)

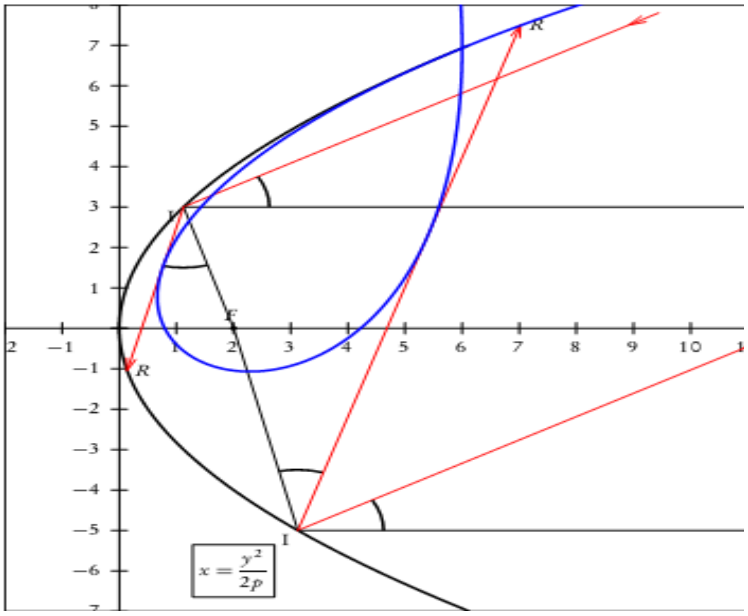

So, $\kappa = \delta - \mu = -\arctan\left(\frac{y_I}{\frac{p}{2} - \frac{y_I^2}{p}}\right) + \pi - \mu$ (A2)

The equation of the reflected ray (IR) is:

$$y = x\tan\kappa + b \tag{A3}$$

Where, $b = y_I - x_I \tan\kappa$ (A4)

Let's derive the equation (A3) in relation to y_I, and it becomes:

$$0 = x(\tan\kappa)' + 1 - \frac{y_I^2}{2p}(\tan\kappa)' - \frac{y_I}{p}\tan\kappa \tag{A5}$$

With, $(\tan\kappa)' = \dfrac{-2p}{\left(p^2 + y_I^2\right)\cos^2\left(\arctan\left(2\dfrac{y_I p}{p^2 - y_I^2}\right) + \mu\right)}$ (A6)

The resolution of equations (A3) and (A5) gives the envelope of the reflected rays.

Details of the discretization of transfer equations

Transfer coefficients by convection, h_{12} and h_{12} on the one hand, and by radiation h_{32} and h_{52} on the other hand are expressed as:

$$h_1 = \frac{(Nu_1 \times k_1)}{D_1} \;;\; h_2 = \frac{2\pi K_{eff}}{\ln\left(\frac{D_3}{D_2}\right)} \;;\; h_3 = \frac{\sigma\pi D_2}{\dfrac{1}{\varepsilon_2} + \dfrac{1-\varepsilon_3}{\varepsilon_3}\left(\dfrac{D_2}{D_3}\right)} \;;\; h_4 = 5.67 + 3.86 \times V \;;\; h_5 = \varepsilon_3 \pi\sigma D_4$$

$h_{12} = h_1 \pi D_1$,

$h_{32} = h_3\left(T_2 + T_3\right)\left(T_3^2 + T_{amb}^2\right)$; $h_{42} = h_4 \pi D_4$ and $h_{52} = h_5\left(T_3 + T_{amb}\right)\left(T_3^2 + T_{amb}^2\right)$

And $h_6 = h_2 + h_{32}$, $h_7 = h_{42} + h_{52}$,

$F_1 = \dfrac{\rho_1 C_1 A_1}{\Delta t}$, $F_2 = \dfrac{\rho_1 C_1 q_V}{\Delta z}$,

$F_3 = F_1 + F_2 + h_{12}$, $F_4 = F_1 T_1(j,n)$, $F_5 = F_2 T_1(j-1, n+1)$ and $F_6 = F_4 + F_5$

$G_1 = \dfrac{\rho_2 C_2 A_2}{\Delta t}$, $G_2 = \dfrac{\lambda_2 A_2}{2\Delta z}$, $G_3 = G_1 + 2G_2 + h_6 + h_{12}$, $G_4 = G_1 T_2(j,n)$,

$G_5 = G_2 T_2(j+1, n+1)$, $G_6 = G_2 T_2(j-1, n+1)$, $G_7 = G_4 + G_5 + G_6 + q_a(j, n+1)$

$H_1 = \dfrac{\rho_3 C_3 A_3}{\Delta t}$, $H_2 = \dfrac{\lambda_3 A_3}{2\Delta z}$ $H_3 = H_1 + 2H_2 + h_6 + h_7$, $H_4 = H_1 T_3(j,n)$

$H_5 = H_2 \times T_3(j+1, n+1)$, $H_6 = H_2 \times T_3(j-1, n+1)$, $H_7 = h_7 \times T_{amb}$, $H_8 = H_7 + q_b(j, n+1)$

$H_9 = H_4 + H_5 + H_6 + H_8$

The discretization of the above system gives:

$$\begin{cases} \rho_1 C_1 A_1\left(\dfrac{T_1(j,n+1)-T_1(j,n)}{\Delta t}\right) = -\rho_1 C_1 q_V\left(\dfrac{T_1(j,n+1)-T_1(j-1,n+1)}{\Delta z}\right) + h_{12}\left(T_2(j,n+1)-T_1(j,n+1)\right) \\ \rho_2 C_2 A_2\left(\dfrac{T_2(j,n+1)-T_2(j,n)}{\Delta t}\right) = \lambda_2 A_2 \dfrac{T_2(j+1,n+1)-2T_2(j,n+1)+T_2(j-1,n+1)}{2\Delta z} + q_a(j,n+1) - h_6\left(T_2(j,n+1)-T_3(j,n+1)\right) - h_{12}\left(T_2(j,n+1)-T_1(j,n+1)\right. \\ \rho_3 C_3 A_3\left(\dfrac{T_3(j,n+1)-T_3(j,n)}{\Delta t}\right) = \lambda_3 A_3 \dfrac{T_3(j+1,n+1)-2T_3(j,n+1)+T_3(j-1;n+1)}{2\Delta z} + h_6\left(T_2(j,n+1)-T_3(j,n+1)\right) - h_7\left(T_3(j,n+1)-T_{amb}\right) + q_b(j,n+1) \end{cases}$$

This leads to the following system:

$$\begin{cases} \left(F_1+F_2+h_{12}\right)T_1(j,n+1) - h_{12}T_2(j,n+1) = F_1T_1(j,n) + F_2T_1(j-1,n+1) \\ -h_{12}T_1(j,n+1) + \left(G_1+2G_2+h_6+h_{12}\right)T_2(j,n+1) - h_6T_3(j,n+1) = G_1T_2(j,n) + G_2T_2(j+1,n+1) + G_2T_2(j-1,n+1) + q_a(j,n+1) \\ -h_6T_2(j,n+1) + \left(H_1+2H_2+h_6+h_7\right)T_3(j,n+1) = H_1T_3(j,n) + H_2T_3(j+1,n+1) + H_2T_3(j-1,n+1) + h_7T_{amb} + q_b(j,n+1) \end{cases}$$

$$\begin{cases} F_3T_1(j,n+1) - h_{12}T_2(j,n+1) = F_4 + F_5 \\ -h_{12}T_1(j,n+1) + G_3T_2(j,n+1) - h_6T_3(j,n+1) = G_4 + G_5 + G_6 + q_a(j,n+1) \\ -h_6T_2(j,n+1) + H_3T_3(j,n+1) = H_4 + H_5 + H_6 + H_7 + q_b(j,n+1) \end{cases}$$

$$\begin{cases} F_3T_1(j,n+1) - h_{12}T_2(j,n+1) = F_6 \\ -h_{12}T_1(j,n+1) + G_3T_2(j,n+1) - h_6T_3(j,n+1) = G_7 \\ -h_6T_2(j,n+1) + H_3T_3(j,n+1) = H_9 \end{cases} \Leftrightarrow \begin{pmatrix} F_3 & -h_{12} & 0 \\ -h_{12} & G_3 & -h_6 \\ 0 & -h_6 & H_3 \end{pmatrix} \begin{pmatrix} T_1(j,n+1) \\ T_2(j,n+1) \\ T_3(j,n+1) \end{pmatrix} = \begin{pmatrix} F_6 \\ G_7 \\ H_9 \end{pmatrix}$$